Communication

Monolithic, Optically Coupled, Multi-Section Mid-IR Quantum Cascade Lasers

Kamil Pierściński *[ID], Dorota Pierścińska, Grzegorz Sobczak [ID], Aleksandr Kuźmicz, Krzysztof Chmielewski [ID], Katarzyna Krajewska [ID] and Piotr Gutowski

Łukasiewicz Instytut Mikroelektroniki i Fotoniki (Ł-IMiF), 02-668 Warsaw, Poland;
dorota.pierscinska@imif.lukasiewicz.gov.pl (D.P.); Grzegorz.Sobczak@imif.lukasiewicz.gov.pl (G.S.);
Aleksandr.Kuzmicz@imif.lukasiewicz.gov.pl (A.K.); krzysztof.chmielewski@imif.lukasiewicz.gov.pl (K.C.);
katarzyna.krajewska@imif.lukasiewicz.gov.pl (K.K.); piotr.gutowski@imif.lukasiewicz.gov.pl (P.G.)
* Correspondence: kamil.pierscinski@imif.lukasiewicz.gov.pl

Abstract: Mid-infrared (mid-IR $\lambda \approx$ 3–12 μm), single-mode-emission Quantum Cascade Lasers (QCLs) are of significant interest for a wide range of applications, especially as the laser sources are chosen for laser absorption spectroscopy. In this work, we present the design, fabrication and characterization of multi-section, coupled-cavity, mid-IR quantum cascade lasers. The purpose of this work is to propose a design modification for a coupled-cavity device, yielding a single-mode emission with a longer range of continuous tuning during the pulse, in contrast to a 2-section device. This effect was obtained and demonstrated in the work. The proposed design of a 3-section coupled-cavity QCL allows for a single-mode emission with 35 dB side-mode suppression ratio. Additionally, the time-resolved spectra of the wavelength shift during pulse operation, show a continuous tuning of ~3 cm^{-1} during the 2 μs pulse. The devices were fabricated in a slightly modified, standard laser process using dry etching.

Keywords: quantum cascade lasers (QCLs); coupled cavities; wavelength tuning

1. Introduction

Single-mode emission is one of the crucial requirements for Quantum Cascade Lasers (QCLs), which are compact laser sources of infrared radiation in the mid-IR range (3–20 μm) and in the THz range (1–5 THz). This feature is particularly important in all spectroscopic applications, such as industrial process monitoring [1], remote sensing [2], breath analysis for medical diagnostics [3], or industrial process monitoring [2].

To date, the literature describes several approaches to obtaining a single-mode emission from QCL, such as distributed feedback (DFB) [4], external cavity (EC) [5], distributed Bragg reflector (DBR) mirrors [6], injection locking [7], very short Fabry–Perot (FP) cavity QCL [8] or photonic crystals resonators [9]. All of these solutions are possible to implement experimentally; however, they either require additional or external elements (e.g., external cavity), thus leading to systems sensitive to mechanical vibrations, or to the high cost of a single device due to the complexity of processing technology (e.g., DFB).

Another solution that is used to achieve a single-mode operation of a laser is monolithically coupled laser cavities. The 2-section coupled-cavity (CC) technique was originally proposed in 1980s by L. A. Coldren et al. [10–12] and successfully applied to an AlGaAs–GaAs interband, multiquantum-well laser. Therefore, a solution based on a monolithically integrated, coupled-cavity design is proposed, which offers a relatively low fabrication complexity while still yielding a single-mode emission. In our previous paper [13], we described a single-mode emission from 2-section CC QCLs fabricated by focused ion beam (FIB) milling or by inductively coupled plasma reactive ion etching (ICP-RIE). These devices were characterized by a stable, single-mode operation and relatively high optical power. Additionally, a high repeatability and high yield were achieved for CC QCLs fabricated by ICP. However, the

devices suffered from relatively low mode-hop-free intrapulse spectral tuning (~1 cm^{-1}). The purpose of this work is to propose a design modification, yielding a device that can emit a single mode with a longer range of continuous tuning during the pulse, in contrast to a 2-section device. This effect was obtained and demonstrated in this work.

To overcome the shortcomings of 2-section devices, we proposed modifying the design by introducing a third section (second optical gap). Based on calculations, it is expected that adding a third section, significantly shorter than the two other sections, will result in an increase in the intrapulse, single-mode tuning range, allowing a wider mode-hop-free tuning range.

In this paper, we proposed a modified approach to coupled-cavity QCLs, based on multisection (3-section) CC QCLs. The range of spectral tuning is very important from the point of view of applications in optical sensing techniques based on the intrapulse tuning of the laser emission [14]. In direct absorption laser spectroscopy, the emission line of the laser source is swept (tuned) across the absorption line or several lines of gas [15,16].

2. Investigated Devices and Fabrication Technology

The investigated devices were AlInAs/InGaAs/InP, lattice-matched QCLs, grown by molecular beam epitaxy (MBE) technology, designed for an emission at ~8.6 μm [17]. The QCL structures were grown using lattice-matched $In_{0.53}Ga_{0.47}As/In_{0.52}Al_{0.48}As$ active regions based on a four-well, two-phonon resonance design. The layer sequence of one period of the structure, in nanometers, starting from the injection barrier, was **4.0**, 1.9, **0.7**, 5.8, **0.9**, 5.7, **0.9**, 5.0, **2.2**, 3.4, **1.4**, 3.3, **1.3**, <u>3.2</u>, **1.5**, <u>3.1</u>, **1.9**, 3.0, **2.3**, 2.9, **2.5**, **2.9** nm. AlInAs layers are denoted in bold. The underlined layers were n doped to 1.5×10^{11} cm^{-2}. The waveguide from the bottom side was formed by a low-doped InP substrate and from the top by a 2.5 μm InAlAs layer covered by a heavily doped InGaAs contact layer [18].

Fabrication technology of 3-section CC QCLs was based on the ICP—RIE technique. The process was a slight modification of the standard fabrication process of double-trench waveguide QCL [13,19].

The fabrication process was similar to the one described reported previously in [13]. A schematic illustration of the device fabrication process is shown in Figure 1. An optical microscope image of a fabricated, 3-section CC QCLs heterostructure is shown in Figure 2. In this paper, the following abbreviations were used when referring sections: short section—SS, middle section—MS, and long section—LS.
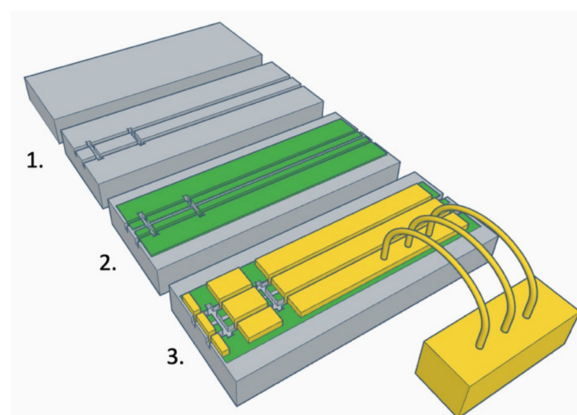

Figure 1. Schematic of 3-section CC QCLs fabrication process: 1. Definition and etching of optical gaps and trenches defining mesa, 2. Deposition of dielectrics, 3. Evaporation of metal contact and bonding.
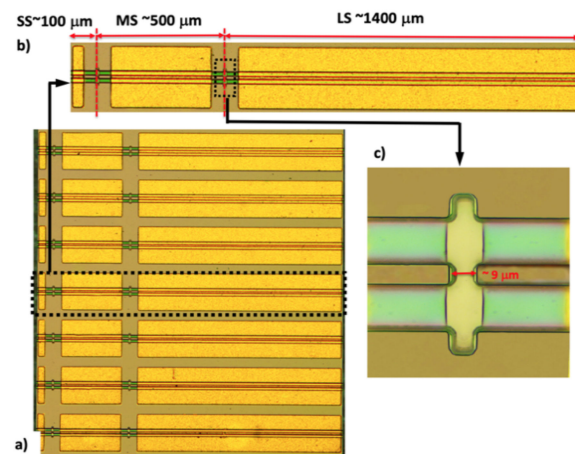
Figure 2. Optical microscope image of a 3-section CC QCLs heterostructure: (**a**) a part of processed epitaxial wafer before cleaving, (**b**) close-up on single chip, and (**c**) close up of the optical gap between MS and LS.

Multicomponent (methane–hydrogen-based) plasma was used for anisotropic etching of the semiconductor heterostructure in the ICP—RIE reactor through a hard mask to define two optical gaps of about 5 µm width simultaneously with mesa. PECVD (Plasma-Enhanced Chemical Vapor Deposition)-deposited, stress-compensated Si_3N_4 dielectric film was "opened" in defined places by F-based dry etching to produce contact windows. The electrical gaps in the vicinity of optical gaps were defined by a "lift-ff" of top contact metallization (Ti/Pt/Au). The resulting contacts were thickened by galvanization to several microns for mechanical robustness. The QCL chip processing was finalized by the chemical–mechanical thinning of the substrate and deposition of lower contact metallization (AuGe/Ni/Au).

3. Experimental Results and Discussion

3.1. Numerical Results

In our previous paper, we used a simple model for coupled cavities, treating them as a system of two separate FP resonators, exhibiting total transmission. In such a system, only the modes that occurred at frequencies (wavelengths) common to both cavities could be transmitted. In other words, only those modes of longer cavities can propagate, which are "selected" by the short cavity. One can think of the short section as the filter that selects specific modes of long cavity. The selected modes are separated by the free spectral range (FSR) of the short cavity. Such simplification of the description yielded results that were in good agreement with experimental data. Our previous results showed that 2-section devices performed well, demonstrating a single-mode operation. However, this design was not appropriate for intrapulse absorption spectroscopy, as the emission exhibited jumps between the modes selected by the short section. This detection method requires the stable tuning of the laser line throughout the pulse duration. Thus, despite single-mode operation, the tuning during the pulse was not continuous. This mechanism is presented in Figure 3. The TRS (time-resolved spectrum) of 2-section CC QCL was registered for a pulse duration of 1 µs. The discontinuity in the spectrum is clearly visible, following the spacing defined by the short-section FSR.
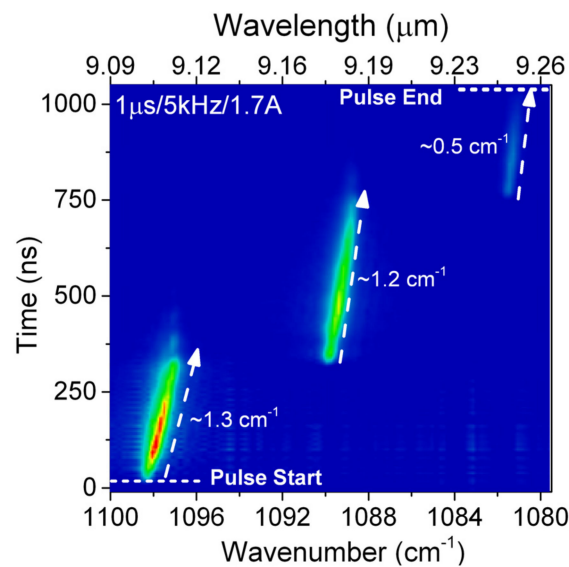
Figure 3. Time resolved wavelength tuning map registered for 2-section CC QCL operated with 1 μs pulses at 5 kHz repetition rate [13]. CC BY 4.0.

Several test structures, with a cavity length of 2 mm and variable lengths of short section, were fabricated; however, no satisfactory results were obtained. In the case of a 2-section device with a high length ratio of LS to SS (i.e., for very short SS), the effect of discrimination of side modes was insufficient due to a relatively broad peak of transmission of SS and smaller FSR of LS. The combination of three factors, namely broad gain, smaller FSR of LS and broad SS transmission peak resulted in the multi-mode operation of device.

Following the conclusions from the experimental and numerical results of 2-section devices, a modification was proposed to increase the mode-hope-free tuning range for single-mode emission of CC QCL. The modification adds the additional selectivity of modes by adding a third section to the system. The third, shortest section should be short enough to have a large spacing between the allowed modes. The FSR of the middle section should be larger than the FSR of the long section. Thus, the pair of modes at the frequencies allowed both in middle and long sections are selected and transmitted by the third, shortest section. The resonances of the system of three cavities will be present at frequencies (wavelengths) defined by the SS frequencies.

The calculated transmission of the system of two and three resonators is shown in Figure 4. In the upper panel of Figure 4, the optical microscope images for the top view of investigated devices are presented; the 2-section device is shown on the left and 3-section device is shown on the right. The location of optical gaps and the ratio of section lengths are visible. The lower panel of Figure 4 shows the transmission of the system of FP cavities (total transmission), as well as transmissions of individual sections.

Figure 4 presents how adding the third, shortest section affects the total transmission of the system. There is a significant difference in the transmission of the system for 2- and 3-section devices. It can be seen that, in case of the 2-section device, the allowed modes of the coupled system are spaced by less than 4 cm^{-1}, in contrast to the 3-section system. The experimental results of 2-section devices showed this separation of the modes in the optical spectrum. In the case of the 3-section device, the side modes that are present in the transmission are separated by the FSR of the shortest section. Thus, the shortest cavity guaranties a single-mode operation by introducing a large separation between the allowed modes of the system. This effect cannot be obtained by the 2-section design without a significant reduction in the length of the long section.
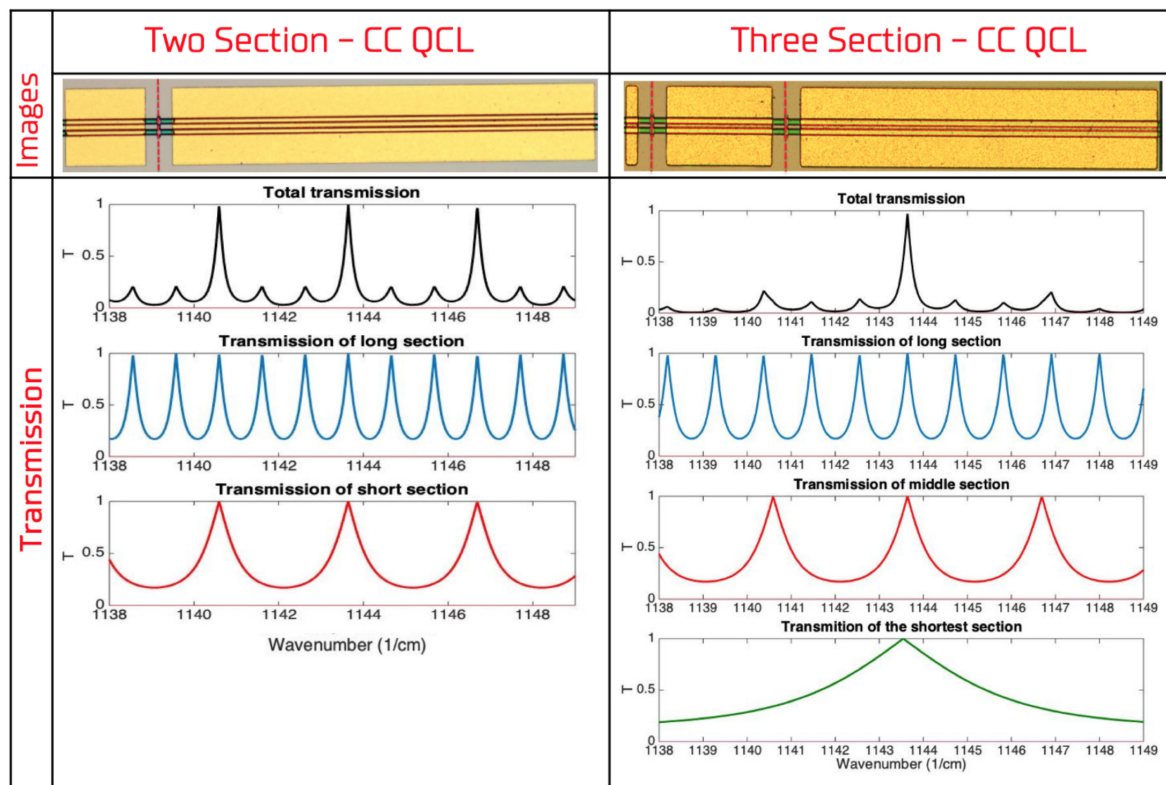
Figure 4. Upper panel: optical images of 2- and 3-section CC-QCLs. Lower panel: calculated transmission of F-P cavities of QCLs: first row composite transmission of 2- and 3-section resonator; second and third rows transmissions of individual sections (short and middle, respectively); fourth transmission of the shortest section in 3-section CC QCL. The section lengths are: 100 μm, 500 μm and 1400 μm, for short, middle and long sections, respectively.

In summary, in the case of 3-section devices, one should expect significantly improved mode-hop-free tuning range and suppression of the mode-hopping mechanism. Based on results of calculations the following section lengths were chosen: 100 μm, 500 μm and 1400 μm, for short, middle and long sections, respectively. Devices following this design were fabricated and characterized.

3.2. Experimental Results

To assess and prove the idea of a 3-section QCL, a series of devices were fabricated. To confirm the performance and spectral behavior of the 3-section devices, detailed measurements were performed. Characterization included standard light-current-voltage (L-I-V) measurements [20], as well as spectral and TRS characterization [21]. Time-resolved spectral measurements were used to specifically characterize the spectral tuning of the emission during the pulse duration. This also demonstrated if the device emitted a single mode during the whole pulse. Such an approach is used to characterize the shift of emission, as an indication of intrapulse absorption spectroscopy applications [22]. Additionally, the results of the temperature tuning of the CC QCLs are presented.

The L-I-V characteristics of investigated 3-section CC QCLs were performed in a standard experimental set-up [23], with a TE-cooled Mercury-Cadmium-Telluride (MCT) detector. The temperature of the device was stabilized at 20 °C to minimize the effect of ambient temperature on spectra and stabilize device parameters. Figure 5a shows L-I-V curves for the device operated in pulse mode with a 200 ns and 5 kHz repetition rate. For comparison, the L-I-V curves for the FP laser are also shown. The FP laser was fabricated from the same wafer in the same fabrication batch. The unmodified, FP device was processed as a ridge waveguide design with a ridge width of 18 μm and 2 mm cavity length. The threshold current of 3-section CC QCL is comparable with the threshold current

of a standard FP laser. This indicates that the introduction of the optical gap and mirrors formed by dry etching does not result in a significant increase in cavity losses. The process of dry etching of the optical gap was carefully optimized to reduce possible losses due to imperfections of the mirror surface. Figure 5b shows the comparison of spectra of an FP cavity device (black line) and 3-section CC QCL (red line). The inset in Figure 5b shows a single-mode operation spectrum of investigated devices measured at a current equal to 1.3 I_{th} presented in a logarithmic scale. The side-mode suppression ratio is 35 dB.
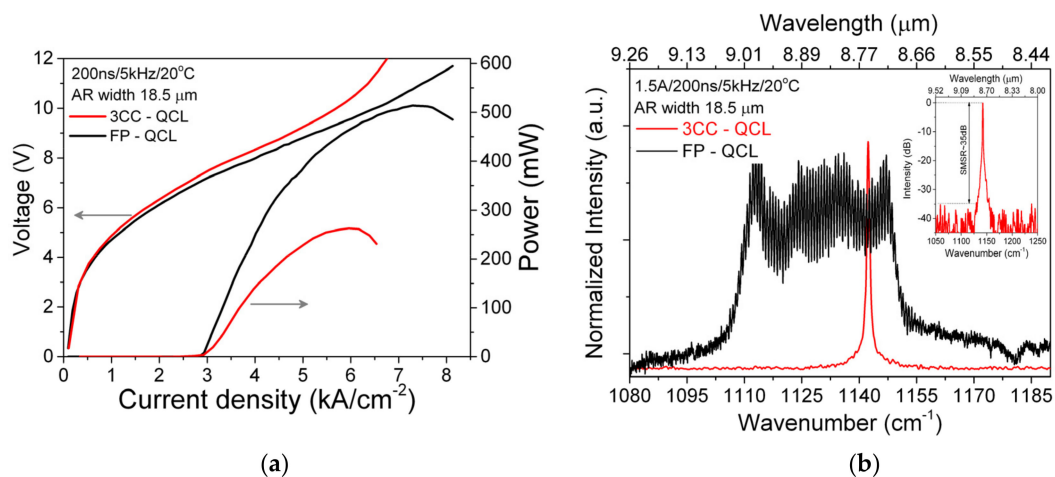

(**a**)   (**b**)

Figure 5. (**a**) L-I-V characteristics of 3-section CC QCL measured at room temperature (red line). For comparison: L-I-V characteristics of F-P device (black line); (**b**) comparison of spectra of 3-section CC QCL (red line) and FP device (black line). Spectra were measured at 1.3 I_{th} (1.5 A) at RT. The inset shows a single-mode operation spectrum measured at 1.3 I_{th} presented in y-log scale showing 35 dB side-mode suppression ratio.

The spectra were measured using Fourier Transform Infrared (FTIR) spectrometer (Nicolet 8700) with a liquid-nitrogen-cooled, photovoltaic MCT infrared detector placed inside the spectrometer. A single-mode operation measured at room temperature for a current of 1.3 I_{th} was recorded at ~1142 cm^{-1} (8.75 μm). Spectra show clean, single-mode emissions with a side-mode suppression ratio (SMSR) of 35 dB (Figure 5b).

3.2.1. Temperature Tuning

To verify that the 3-section QCL emits a stable single mode at various temperatures of operation, temperature tuning measurements were performed. The temperature of the device was changed by the TE element in the range from 10 °C to 90 °C. Figure 6 presents spectra registered at different temperatures. A single-mode emission was observed in the whole temperature range. The total tuning range was ~7 cm^{-1}, resulting in a temperature tuning coefficient of 0.08 cm^{-1}/K. Spectra show no indication of side modes switching on during operation at elevated temperatures.

3.2.2. Intrapulse Tuning-Time Resolved Spectra

To record how the optical pulse evolves during the pulse, TRS measurements were performed. TRS spectra were registered for different pulse durations: 200 ns, 500 ns, 1 μs and 2 μs.

Figure 7 presents TRS spectra vs. pulse duration. In all cases, a 3-section CC QCL emits a single mode with no mode hopping. Additionally, no evidence of side modes is visible. This result experimentally confirms that introducing the third section improves the stability of the device in terms of the mode-hop-free wavelength tuning.
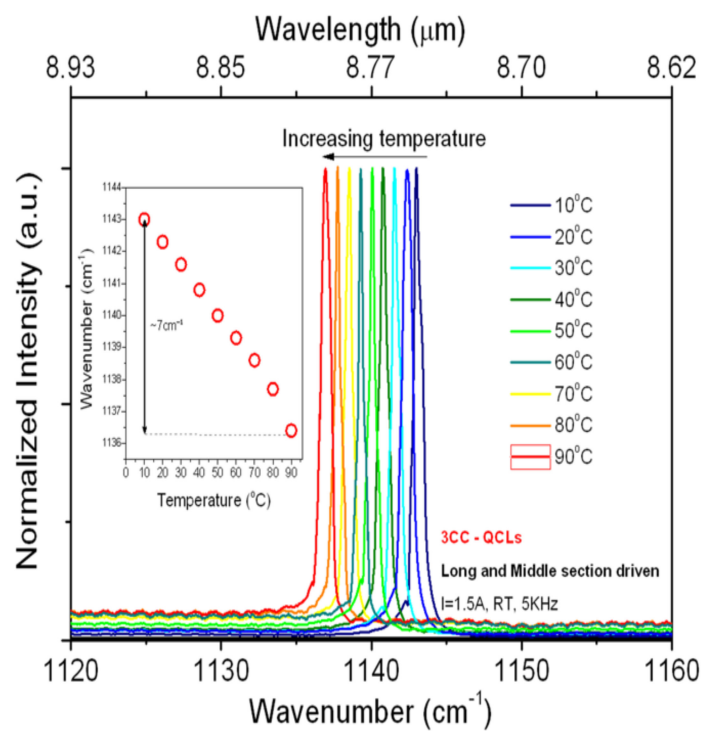
Figure 6. Emission spectra of 3-section CC QCL operated at a constant current 1.3 I_{th} and various heat sink temperatures. Inset shows the single-mode emission shift: wavenumber vs. heat sink temperature.

Figure 7. Emission spectra of 3-section CC QCL operated at a constant current 1.3 I_{th} and various heat sink temperatures. Inset shows the single-mode emission shift: wavenumber vs. heat sink temperature.
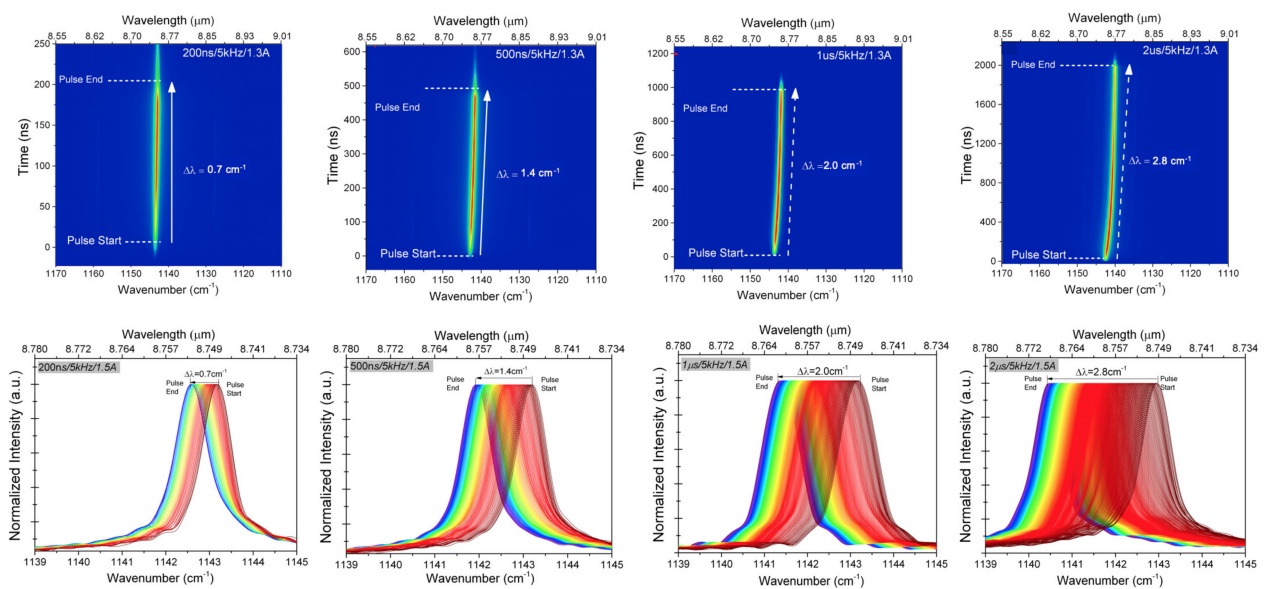
The lower row in Figure 7 shows normalized spectra extracted from the map. The TRS mode of spectral measurements is particularly well-suited for the characterization of light-emitting devices that undergo tuning during the operation. As the spectrum registered in rapid or step-scan modes is an averaged snapshot of the optical pulse, it appears broadened, or even in a multimode, depending on the resolution of the spectrometer and device design.

Figure 8 presents the tuning of the optical spectra for various pulse durations extracted from data presented in Figure 7. In case of the longest pulses, it can be observed that the

wavelength shift is nonlinear in time, as is expected considering the thermal properties of semiconductor lasers.
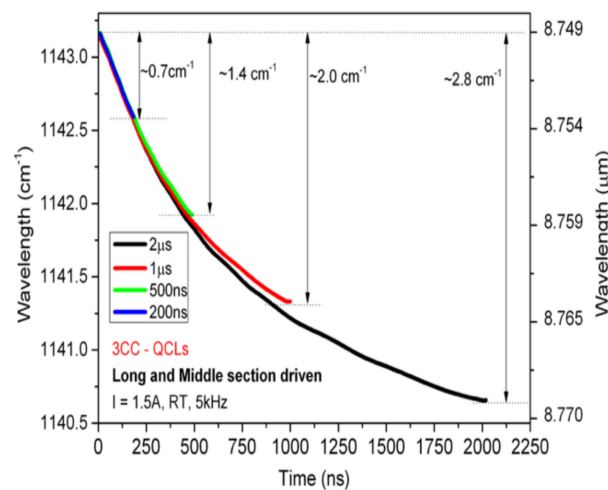

Figure 8. Tuning of the wavelength as extracted from the emission TRS spectra of 3-section CC QCL operated at a constant current of 1.3 I_{th}. The tuning rates are presented for various pulse durations.

Figure 9 presents a comparison of time-resolved experimental spectra and the calculated transmission of a system composed of three FP cavities. The tuning of transmission during the pulse was realized by assuming the change of refractive index. Calculations were performed to show how the transmission spectrum changes with the change of the effective refractive index for 3-section QCLs. The linear variation of the refractive index was assumed for the calculations. This calculation represents thermal tuning occurring during pulse (internal heating) or the change in the temperature of the device (external heating).
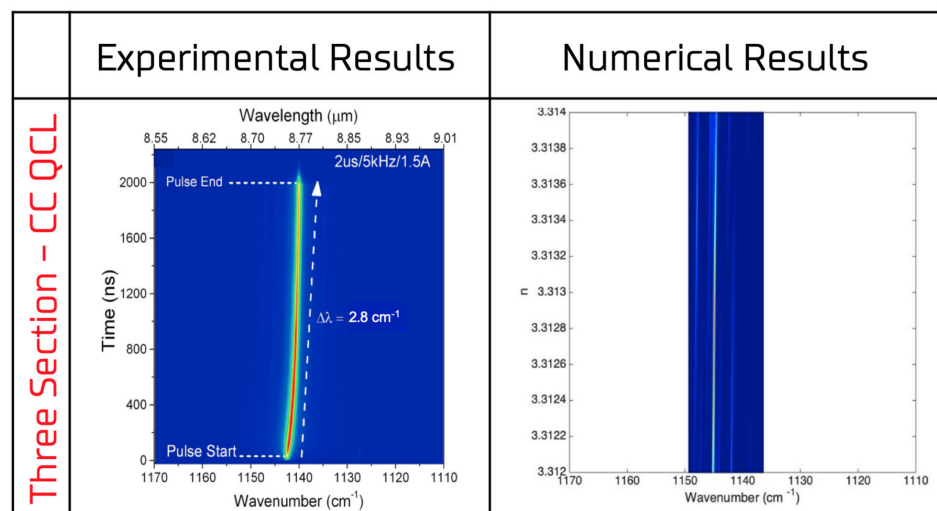

Figure 9. Comparison of experimentally registered emission spectrum of 3-section CC QCL and numerically calculated transmission of three F-P elements system.

4. Conclusions

In this work we introduced a modified, coupled-cavity device, consisting of three sections, with two optical gaps. This modification yielded devices emitting a single mode with a longer range of continuous tuning during the pulse, in contrast to a 2-section device. This effect was demonstrated and characterized in the work. We designed and fabricated a 3-section CC QCLs offering continuous intrapulse wavelength tuning, as opposed to a 2-section design, which

we proposed and fabricated in previous work. The total tuning of 2.8 cm^{-1} was obtained for a 2 μs pulse width. The device operates at elevated temperatures. The improvement in the range of continuous spectral tuning for a 3-section device is compared to a 2-section laser. The third section significantly improved the performance of the laser in terms of the range of mode-hop-free intrapulse wavelength tuning.

Author Contributions: K.P.: Conceptualization, methodology, investigation, data curation, formal analysis, visualization, funding acquisition, writing—review and editing of the manuscript, D.P. and G.S.: investigation, methodology and visualization, A.K. and K.C.: investigation (fabrication of devices), K.K.: investigation, P.G.: Investigation (structure growth). All authors discussed results and contributed to the formulation of conclusions. All authors have read and agreed to the published version of the manuscript.

Institutional Review Board Statement: Not applicable.

Informed Consent Statement: Not applicable.

Data Availability Statement: The data that support the findings of this study are available from the corresponding author upon reasonable request.

Conflicts of Interest: The authors declare no conflict of interest.

References

1.　Curl, R.F.; Capasso, F.; Gmachl, C.; Kosterev, A.A.; McManus, B.; Lewicki, R.; Pusharsky, M.; Wysocki, G.; Tittel, F.K. Quantum cascade lasers in chemical physics. *Chem. Phys. Lett.* **2010**, *487*, 1–18. [CrossRef]

2.　Sydoryk, I.; Lim, A.; Jäger, W.; Tulip, J.; Parsons, M.T. Detection of benzene and toluene gases using a Mid infrared continuous-wave external cavity quantum cascade laser at atmospheric pressure. *Appl. Opt.* **2010**, *49*, 945–949. [CrossRef] [PubMed]

3.　Schwaighofer, A.; Brandstetter, M.; Lendl, B. Quantum cascade lasers (QCLs) in biomedical spectroscopy. *Chem. Soc. Rev.* **2017**, *46*, 5903–5924. [CrossRef] [PubMed]

4.　Wittmann, A.; Bonetti, Y.; Fischer, M.; Faist, J.; Blaser, S.; Gini, E. Distributed-Feedback Quantum-Cascade Lasers at 9 um Operating in Continuous Wave up to 423 K, IEEE Photon. *Technol. Lett.* **2009**, *814*, 21.

5.　Hugi, A.; Maulini, R.; Faist, J. External cavity quantum cascade laser, Semicond. *Sci. Technol.* **2010**, *083001*, 25.

6.　Cheng, L.; Choa, F.-S. Design and operation of mid-IR integrated DBR tunable lasers. *Proc. SPIE* **2011**, *7953*, 79531p.

7.　Wang, C.; Grillot, F.; Kovanis, V.; Even, J. Rate equation analysis of injection-locked quantum cascade lasers. *J. Appl. Phys.* **2013**, *063104*, 113. [CrossRef]

8.　Hofling, S.; Reithmaier, J.; Forchel, A. Device performance and wavelength tuning behavior of ultra-short quantum-cascade microlasers with deeply etched Bragg-mirrors. *IEEE J. Sel. Top. Quantum Electron.* **2005**, *11*, 1048–1054. [CrossRef]

9.　Colombelli, R.; Srinivasan, K.; Troccoli, M.; Painter, O.; Gmachl, C.F.; Tennant, D.M.; Sergent, A.M.; Sivco, D.L.; Cho, A.Y.; Capasso, F. Quantum cascade surface-emitting photonic crystal laser. *Science* **2003**, *302*, 1374–1377. [CrossRef]

10.　Coldren, L.A.; Miller, B.I.; Iga, K.; Rentschler, J.A. Monolithic two-section GaInAsP/InP active-optical resonator devices formed by reactive ion etching. *Appl. Phys. Lett.* **1981**, *38*, 315–317. [CrossRef]

11.　Coldren, L.A.; Koch, T.L. Analysis and design of coupled-cavity lasers—Part I: Threshold gain analysis and design guidelines. *IEEE J. Quantum Electron.* **1984**, *20*, 659–670. [CrossRef]

12.　Coldren, L.A.; Koch, T.L. Analysis and design of coupled-cavity lasers—Part II: Transient analysis. *IEEE J. Quantum Electron.* **1984**, *20*, 671–682. [CrossRef]

13.　Pierściński, K.; Pierścińska, D.; Kuźmicz, A.; Sobczak, G.; Bugajski, M.; Gutowski, P.; Chmielewski, K. Coupled Cavity Mid-IR Quantum Cascade Lasers Fabricated by Dry Etching. *Photonics* **2020**, *7*, 45. [CrossRef]

14.　Mikołajczyk, J.; Bielecki, Z.; Stacewicz, T.; Smulko, J.; Wojtas, J.; Szabra, D.; Prokopiuk, A.; Magryta, P. Detection of Gaseous Compounds with Different Techniques Metrol. *Meas. Syst.* **2016**, *23*, 205–224. [CrossRef]

15.　Nadeem, F.; Mandon, J.; Khodabakhsh, A.; Cristescu, S.M.; Harren, F.J.M. Sensitive Spectroscopy of Acetone Using a Widely Tunable External-Cavity Quantum Cascade Laser. *Sensors* **2018**, *18*, 2050. [CrossRef]

16.　Wojtas, J.; Bielecki, Z.; Stacewicz, T.; Mikolajczyk, J.; Medrzycki, R.; Rutecka, B. Application of quantum cascade lasers in nitric oxide and nitrous oxide detection. *Acta Phys. Pol. A* **2011**, *4*, 794–797. [CrossRef]

17.　Gutowski, P.; Karbownik, P.; Trajnerowicz, A.; Pierściński, K.; Pierścińska, D.; Sankowska, I.; Kubacka-Traczyk, J.; Sakowicz, M.; Bugajski, M. Room temperature AlInAs/InGaAs/InP quantum cascade lasers. *Photonics Lett. Pol.* **2014**, *6*, 142–144.

18. Gutowski, P.; Sankowska, I.; Słupiński, T.; Pierścińska, D.; Pierściński, K.; Kuźmicz, A.; Gołaszewska-Malec, K.; Bugajski, M. Optimization of MBE Growth Conditions of In$_{0.52}$A$_{l0.48}$As Waveguide Layers for InGaAs/InAlAs/InP Quantum Cascade Lasers. *Materials* **2019**, *12*, 1621. [CrossRef]

19. Bugajski, M.; Gutowski, P.; Karbownik, P.; Kolek, A.; Hałdaś, G.; Pierściński, K.; Pierścińska, D.; Kubacka-Traczyk, J.; Sankowska, I.; Trajnerowicz, A.; et al. Mid-IR quantum cascade lasers: Device technology and non-equilibrium Green's function modeling of electro-optical characteristics. *Phys. Status Solidi (B)* **2014**, *251*, 1144–1157. [CrossRef]

20. Pierścińska, D.; Pierściński, K.; Iwińska, M.; Kosiel, K.; Szerling, A.; Karbownik, P.; Bugajski, M. Electrical and optical characterization of mid-IR GaAs/AlGaAs quantum cascade lasers. *Proc. SPIE* **2012**, *8432*, 84321S.

21. Pierściński, K.; Pierścińska, D.; Szabra, D.; Nowakowski, M.; Wojtas, J.; Mikołajczyk, J.; Bielecki, Z.; Bugajski, M. Time resolved FTIR study of spectral tuning and thermal dynamics of mid-IR QCLs. *Proc. SPIE* **2014**, *9134*, 91341L.

22. Gadedjisso-Tossou, K.S.; Stoychev, L.I.; Mohou, M.A.; Cabrera, H.; Niemela, J.; Danailov, M.B.; Vacchi, A. Cavity Ring-Down Spectroscopy for Molecular Trace Gas Detection Using A Pulsed DFB QCL Emitting at 6.8 μm. *Photonics* **2020**, *7*, 74. [CrossRef]

23. Pierściński, K.; Bugajski, M.; Czyszanowski, T.; Kolek, A.; Wesołowski, M.; Kuc, M.; Sarzała, R.P.; Dems, M.; Płuska, M.; Pierścińska, D.; et al. Coupled-cavity AlInAs/InGaAs/InP quantum cascade lasers fabricated by focused ion beam processing. *J. Phys. Photonics* **2019**, *1*, 015001. [CrossRef]